

Parallel fabrication of high-aspect-ratio all-silicon grooves using femtosecond laser irradiation and wet etching

This content has been downloaded from IOPscience. Please scroll down to see the full text.

2015 J. Micromech. Microeng. 25 115001

(<http://iopscience.iop.org/0960-1317/25/11/115001>)

View [the table of contents for this issue](#), or go to the [journal homepage](#) for more

Download details:

This content was downloaded by: liheyang

IP Address: 202.117.17.127

This content was downloaded on 10/12/2015 at 06:02

Please note that [terms and conditions apply](#).

Parallel fabrication of high-aspect-ratio all-silicon grooves using femtosecond laser irradiation and wet etching

Yanna Li^{1,3}, Tao Chen¹, An Pan¹, Cunxia Li² and Litie Tang³

¹ Key Laboratory for Physical Electronics and Devices of the Ministry of Education & Shaanxi Key Lab of Information Photonic Technique, School of Electronics and Information Engineering, Xi'an Jiaotong University, 28 Xianning West Road, Xi'an 710049, People's Republic of China

² Department of Applied Physics, Xi'an University of Technology, 58 Yanxiang Road, Xi'an 710054, People's Republic of China

³ Northwest Institute of Nuclear Technology, Xi'an, Shaanxi 710024, People's Republic of China

E-mail: Tchen@mail.xjtu.edu.cn

Received 17 March 2015, revised 26 June 2015

Accepted for publication 13 July 2015

Published 25 September 2015



Abstract

This paper introduces a simple method using 800 nm femtosecond laser irradiation and wet etching with a hydrofluoric (HF) acid solution for the parallel fabrication of high-aspect-ratio all-silicon groove arrays. In this method, one laser beam was divided into five beams by a diffractive optical element. Five laser-induced structure change (LISC) zones were formed in the silicon simultaneously with a single scan of the divided beams, and then the materials in the LISC zones were etched by HF acid solution to form groove arrays. Via this method, all-silicon grooves with aspect ratios up to 39.4 were produced, and the processing efficiency could be increased by five times in contrast with that of the single laser beam irradiation. Furthermore, high-aspect-ratio grooves with near uniform morphologies were fabricated using this method in silicon wafers with different crystal orientations.

Keywords: silicon groove, wet etching, parallel fabrication, femtosecond laser

(Some figures may appear in colour only in the online journal)

1. Introduction

Monocrystalline silicon, which is the basic material in the electronic semiconductor field, plays an important role in the semiconductor industry. Silicon-based microstructures, such as high-aspect-ratio grooves [1, 2], micro-spikes [3], and micro-ripples [4], have inspired increasing research interest due to their important potential application in areas such as micro-fluidic devices [5, 6], solar energy cells [7], near-infrared photodetectors [8, 9] and so on.

As one of the silicon-based microstructures, high-aspect-ratio grooves have been successfully applied in a deep silicon insulation trench [10], micro-sensors [6], photonic crystal structures [11, 12] and micro-chemical reactors [13]. Plasma etching is usually employed to produce silicon grooves. However, plasma etching [14, 15] has some drawbacks such

as a high cost, a strict machining environment and the need to use masks. Meanwhile, chemical wet etching [16, 17] is also an effective approach to fabricate silicon grooves. Potassium hydroxide (KOH) and sodium hydroxide (NaOH) are commonly employed as etchants in wet etching. The etching rate on the crystal plane of (100) and (110) is faster than that on the (111) plane in a KOH or NaOH solution, therefore only silicon with special crystal orientations, for example (110)-oriented silicon, can be applied for fabricating deep grooves with a high-aspect ratio. In addition, this method needs an etch barrier which should be removed after etching. This adds complexities to the fabricating process. Based on the anisotropic wet etching of *n*-type (110) silicon wafers in KOH, Tolmachev *et al* fabricated one-dimensional (1D) photonic crystals with 57 μm deep grooves [16]. Dwivedi *et al* fabricated 400 μm deep microchannels in *n*-type (110) silicon

wafers for heat dissipation of semiconductor devices, and found that the aspect ratio of the grooves was less than 6 [18].

In the last few decades, the femtosecond laser has become a powerful tool in areas of ultrafast dynamics measurements [19, 20] and micromachining [21–24]. As an effective way for fabricating microstructures, the femtosecond laser has been used extensively to process a wide range of materials, such as semiconductors [21], polymers [22], glasses [23], and ceramics [24]. Until now, silicon grooves with an aspect ratio of 10 were produced by using femtosecond laser direct writing [25]. However, the debris produced during laser drilling would scatter the subsequent laser pulses and block the energy transfer deeper into the silicon [26, 27]. Therefore high energy was needed for the fabrication of deep silicon grooves. Sven Döring *et al* studied the dependence of the groove depth and width on the laser power and attained a 210 μm deep hole in the silicon using a 50 μJ femtosecond laser [21]. In addition, oxygen species were incorporated into laser-induced structure change (LISC) zones, which is not beneficial for the groove structures which are to be applied in semiconductor devices and micro-electro-mechanical-systems (MEMS).

Recently, it has been reported that high-aspect-ratio LISC zones along the laser transmission direction could be induced inside silicon wafers by a 800 nm femtosecond laser. Elemental analysis results indicate that oxygen species were incorporated into the silicon substrates and SiO_x was formed in the LISC zones [28]. Furthermore, a simple approach for micromachining silicon grooves was proposed in [29]. In this approach, materials in the LISC zones were removed by chemical selective etching, and silicon grooves with an aspect ratio of 16 were produced. Because debris was hardly produced in the LISC zones inside the silicon, this method could avoid the energy loss arising from debris scattering in the laser direct writing groove process. In addition, only silicon species were detected in the grooves and the all-silicon grooves were fabricated after etching. However, the fabrication efficiency was restricted by the scanning velocity, especially for fabricating a groove array, in which the grooves were produced one by one. Parallel fabrication with multi laser beams could highly improve the processing efficiency, which can be achieved by dividing the incident laser beam into multiple beams using diffractive optical elements (DOE) [30, 31]. Laser energy could be utilized more effectively using parallel fabrication techniques. In addition, the parallel fabrication method could be used to pattern the array directly by designing the distribution pattern of the beams. Most importantly, the distribution pattern of the beams produced by the DOE was stable and all the beams reacted with the target simultaneously. Therefore, compared with single beam fabrication, parallel fabrication could decrease the non-uniformity of the array elements arising from laser fluence fluctuation and stage vibration in moving.

In this paper, we introduce a simple method for the parallel fabrication of high-aspect-ratio all-silicon groove arrays using 800 nm femtosecond laser irradiation and wet etching with a hydrofluoric (HF) acid solution. An 800 nm femtosecond laser beam was divided into five beams by a DOE and then was focused onto the silicon wafers by a lens. Five parallel LISC

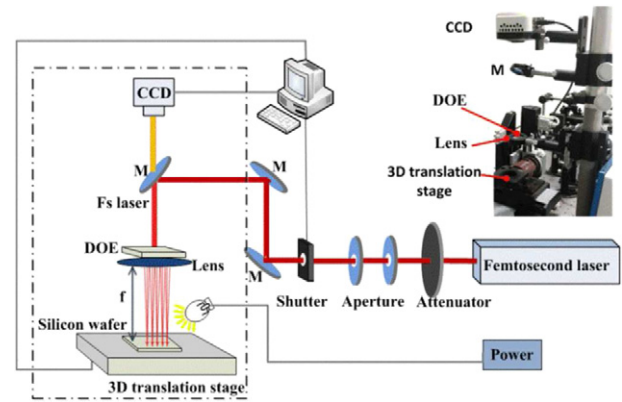


Figure 1. Schematic setup for parallel fabrications of the silicon-based grooves. The inset is the photograph of the marked portion in the dotted box.

zones were formed in the silicon simultaneously by scanning the laser focus over the silicon surface. Then materials in the LISC zones were removed via the HF acid selective etching and five grooves with a near uniform morphology were formed simultaneously. Grooves with aspect ratios up to 39.4 were attained by optimizing femtosecond laser irradiation parameters. The machining efficiency can be improved by five times compared with single beam machining. What is more, high-aspect-ratio grooves with similar morphologies were fabricated in (100)-, (110)- and (111)-oriented silicon wafers. This indicates that this parallel fabrication method is applicable for the fabrication of high-aspect-ratio grooves in various crystal-oriented silicon wafers.

2. Experimental details

Figure 1 shows the schematic setup for the parallel fabrication of the silicon-based grooves using a femtosecond laser and a DOE. An amplified Ti: sapphire femtosecond laser system (Coherent Inc., USA) was used to provide 50 fs laser pulses with a 800 nm central wavelength and a 1 kHz repetition rate. The maximal output power was approximately 3.5 W. The femtosecond laser beam was divided into five laser beams with the same intensities by an eight-level phase modulating DOE. The diameter of each laser beam was approximately 8 mm. Samples were fixed horizontally on a computer-controlled three dimensional (3D) translation stage. Behind the DOE, five laser beams were focused onto the surface of the silicon wafer by a lens. The focal length of the lens was 60 mm. The numerical aperture (NA) was estimated to be approximately 0.07 and the diameter at the focal plane was estimated to be approximately 9.4 μm . The power of the incident laser could be continuously varied by a variable attenuator, and the access of the laser beam was controlled by a mechanical shutter connected to a computer. The pulse duration of the samples was optimized by adjusting the pulse compressor in the laser system and was estimated to be less than 70 fs using the optical Kerr shutter method [20]. A charge coupled device (CCD) camera was used to monitor the laser treating process on line.

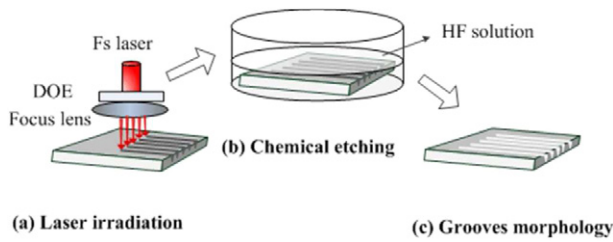


Figure 2. Schematic diagram for the process of the silicon-based grooves fabrication.

As shown in figure 2, there were two steps for the parallel fabrications of silicon-based groove arrays, consisting of laser irradiation and chemical selective etching. Firstly, five LISC zones were induced in the silicon simultaneously using five laser beams produced by a DOE, as shown in figure 2(a). The scanning velocity, scanning length, separation distance and focus position could be varied by controlling the 3D translation stage motion. Secondly, the irradiated silicon wafers were put into a 20 wt% HF acid solution for 2h in an ultrasonic cleaner. Materials in the LISC zones were removed by selective etching to form grooves. Because the silicon material was opaque to visible light, the irradiated silicon wafers were polished with abrasive papers to a random position to observe the laser-induced microstructures in the silicon from the cross section. The samples were polished again after the HF etching to random positions along the laser scanning direction to observe the cross-sectional morphologies of the formed grooves. After polishing, the wafers were ultrasonically cleaned by ethanol and de-ionized water for 15 min each. In our experiments, a scanning electron microscopy (SEM, FEI Quanta 250 FEG Series) equipped with an energy dispersive x-ray spectroscopy (EDS) was employed to characterize the morphologies and the chemical compositions of the LISC and the silicon grooves. The aspect ratio of the grooves was defined as the depth-width ratio. The depth and width were the average depth and width at the half depth of the grooves accordingly.

3. Results and discussion

Figure 3 shows the cross-sectional SEM images of the LISC zones and the chemical selective etching induced grooves. A *p*-type (100) silicon wafer with a thickness of 500 μm was used as the sample. The incident laser power and scanning velocity were set at 75 mW and 2 $\mu\text{m s}^{-1}$, respectively. The scanning length was 500 μm .

As shown in the dotted box of figure 3(a), after 800 nm femtosecond laser irradiation, five LISC zones were induced simultaneously at the irradiated zones along the laser transmission direction. The average depths of the LISC zones (the distance between the top surface and the last laser-induced microcavity in the LISC zones) were approximately 208 μm . The distance between each LISC zone was approximately 120 μm . According to EDS analysis, it could be detected that oxygen was incorporated into the interior of the silicon substrates. The oxygen concentration decreased with the increase in depth. The atomic percentage of oxygen at the top was

approximately 37%, and decreased to 22% at a depth of 164 μm . At the end of the LISC region, the oxygen concentration was 0%. When the irradiated silicon wafers were put into the HF acid solution, materials in the LISC zones were removed and then the grooves were formed. The cross-sectional SEM images of grooves are shown in figure 3(b). It can be seen that there is good uniformity of the grooves. The average depth and width of the grooves were 224 μm and 6.2 μm , respectively. The groove aspect ratio was calculated to be approximately 36.1. The depth difference between the grooves and the LISC zones might arise from the fact that the sample was polished on its side surface after etching to observe the cross-sectional shape of the grooves, and also from the fact that the LISC zone depth fluctuated at different positions. In addition, measurement errors also contributed to the depth difference, because sometimes it was difficult to distinguish the end of the LISC.

According to the above results, the application of the DOE-based parallel fabrication method had the laser scanning time per micrometer decreased from 0.5 s to 0.1 s as compared to using single beam scanning. The etching time was 2h for attaining deep grooves of over 200 μm . After the etching time was taken into account, it took 0.3 s to realize long grooves per micrometer. When a large number of grooves were fabricated, the etching time may be negligible as compared to the laser scanning time. Hence, the processing time for the grooves per micrometer was decreased to 0.1 s. The divided laser beam could be increased to more than five by changing the design of the DOE to increase the production efficiency of the grooves further. In fact, different diffraction angles exist with the beams produced by the DOE, because the DOE beam splitter was based on a diffraction effect. For the configuration in figure 1, only one beam would be incident on the sample normally. As the number of beams increased, the diffraction angles of the outermost beams also increased. We found the entrance of laser ablated holes would become elliptical when the incident angle was over 1 degree and the LISC zones became slightly oblique. In addition, the separation angle between the adjacent beams should be larger than 0.02 degrees to avoid the overlap of adjacent grooves for the 60 mm focal-length lens. Therefore the maximal beam numbers were estimated to be less than 101. For the 101-beam case, the laser power of approximately 1.52W was needed to fabricate grooves with a depth over 200 μm , which was in the output power range of our laser system. Therefore the diffraction angle was the dominantly limiting factor for the maximal beam numbers.

The formation mechanism of the silicon grooves could be attributed to the chemical reaction between the HF acid and SiO_x formed by the femtosecond laser irradiation [32]. When the silicon wafers were irradiated by the femtosecond laser pulses, oxygen species in the ambient air were incorporated into the interior of the silicon substrates and the high-aspect-ratio LISC zones were formed. As shown in figure 3, x was approximately 0.6 for the oxygen atomic percentage of 37% at the top of the LISC zones. x decreased to 0 at the end of the LISC zones, corresponding with pure silicon. The doping depth of the oxygen could be increased with the decrease in the scanning velocity and the increase in the laser power. The NA

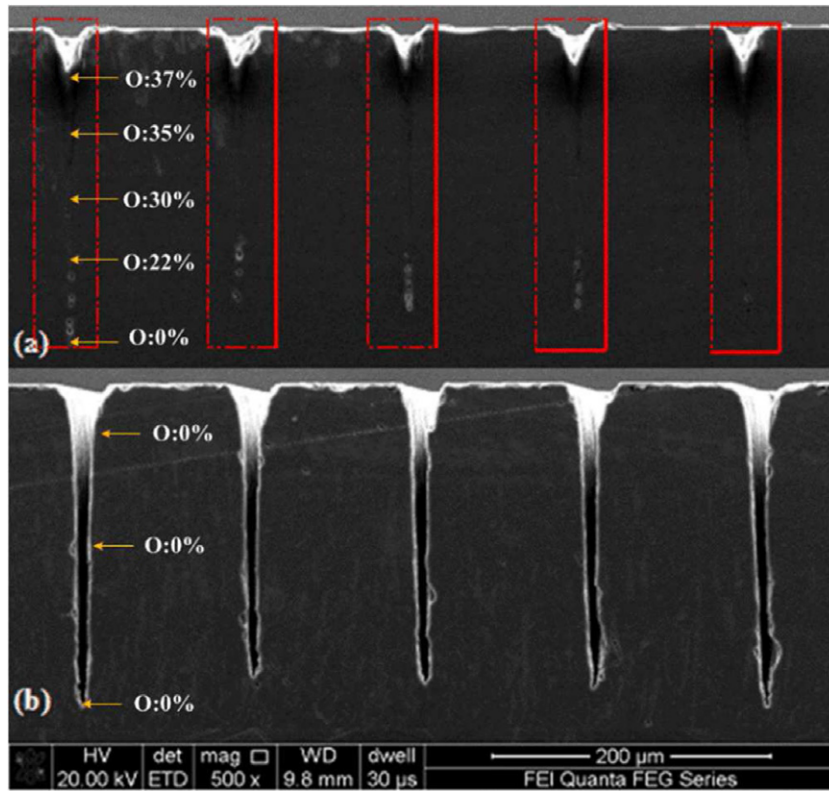


Figure 3. The SEM images of (a) the LISC zones and (b) the chemical selective etching induced grooves, and the atomic percentages of oxygen at different depths.

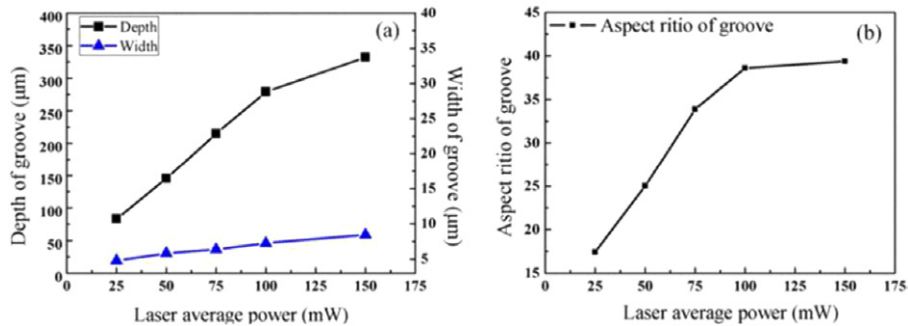


Figure 4. Influences of laser average power on (a) the groove depths and widths, and (b) the aspect ratios.

determined the Rayleigh length of focused light and thereby influenced the depth of the LISC. When the irradiated silicon wafers were put into the HF acid solution, the HF acid reacted with SiO_x in the LISC zones. However, the HF acid hardly reacted with the silicon at room temperature [29]. Therefore only materials in the LISC zones were removed in etching. It implies that the etching was highly selective. During etching, because the entrance of the groove was very narrow, the rate of the fresh acid solution flowing into the groove bottom became low as the groove depth increased. In addition, the oxygen ratio also decreased. Therefore the etch rate would decrease with the increase of the etching time. High-aspect-ratio grooves were produced after removing materials in the LISC zone due to the selective etching. Since grooves were formed only in the LISC zones, the groove depth and width were dependent on the laser power, scanning velocity and the NA of the lens.

In order to study the influence of laser power on the aspect ratios of grooves, we fabricated grooves at different laser powers. The scanning velocity was set at $2 \mu\text{m s}^{-1}$. Figure 4 demonstrates the dependence curve of the depths, widths and aspect ratios of the grooves versus the laser power. When the laser power increased from 25 to 100 mW, the depth, width and aspect ratio of the grooves r increased with the increase in the laser power. At the laser power of 100 mW, grooves with a depth of $279 \mu\text{m}$ and an aspect ratio of 38.6 were attained. When the laser power increased to 150 mW, the depth increased to $332 \mu\text{m}$ and the increase of depth showed a little saturation. The aspect ratio of the grooves increased to 39.4 and became saturated. The aspect ratio and the depth of the grooves were almost two times larger than those in [29]. In our experiments, the laser fluence was about 39.1 J cm^{-2} for the laser power of 150 mW, which was higher than 11.9 J cm^{-2} as detailed in [29]. The application of a lower scanning

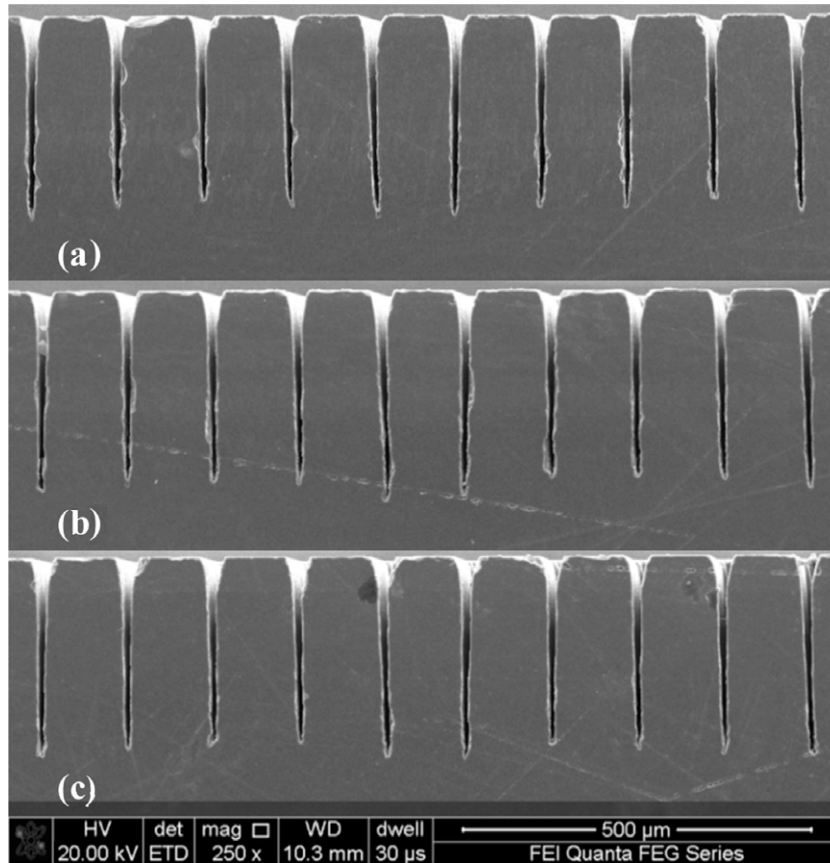


Figure 5. Cross-sectional SEM-images of the grooves in the silicon wafer with different crystal orientations. (a) *p*-type (100), (b) *p*-type (110), and (c) *n*-type (111).

velocity and lenses with more optimal NA also contributed to the improvement of the aspect ratio as compared to that in [29]. The formation of the high-aspect-ratio grooves could be attributed to the self-trapped filament of femtosecond laser that occurred in the LISC region [29]. With the increase in the depth, the absorption increased. The laser power has to be increased to increase the depth of the LISC. However, when the laser power was too high, other complicated nonlinear optical phenomena can occur, for example nonlinear scattering. In addition, the light propagation direction can be disturbed by the asymmetry of the top LISC zones and deviate from the original direction at high depth. Therefore self-trapped filaments of the femtosecond laser would be disturbed in a high depth position and the depth of the LISC zones and grooves could not be increased.

We further investigated the influence of the silicon crystal orientation on the morphologies of grooves formed by this parallel fabrication method. The *p*-type (100), *p*-type (110), *n*-type (111) silicon wafers with thicknesses of 500 μm were used. The incident laser power was set at 100 mW to avoid the saturation of the aspect ratio of the grooves, and the scanning velocity of the laser was set at 2 $\mu\text{m s}^{-1}$. For each sample, the laser beam was scanned two times and the separation distance between each scan was set at 600 μm . Hence ten LISC zones with a period of 120 μm were formed in the silicon wafer accordingly. According to the EDS analysis, the oxygen ratio was almost the same for the three samples. The oxygen atomic

percentage was approximately 41% at the top of the LISC zones, which corresponded to $x = 0.7$. The oxygen atomic percentage decreased to zero at the end of the LISC zones, in which the depth was approximately 270 μm .

The morphologies of the grooves fabricated in the three samples are shown in figure 5. Grooves formed in the silicon wafers with different crystal orientations show similar morphologies. Figure 5(a) shows the cross-sectional SEM-images of the groove arrays in the *p*-type (100) silicon wafer. The average depth and width of the grooves were 276 μm and 7.3 μm , respectively. Figure 5(b) shows the cross-sectional SEM-images of grooves in the *p*-type (110) silicon wafer. The average depth and width of the grooves were 279 μm and 7.2 μm , respectively. For grooves in the *n*-type (111) silicon wafer as shown in figure 5(c), the average depth and width of the grooves were 279 μm and 7.4 μm , respectively. The groove aspect ratios for the three samples were all approximately 39. It can be seen that although the crystal orientations of the silicon wafers were different, the fabricated grooves were almost the same for the same laser irradiation parameters. In other words, this parallel fabrication method is applicable for various crystal-oriented silicon wafers.

The formation of silicon grooves was attributed to the targeted reaction of the oxygen-containing regions and the HF acid solution, so the area of the chemical selective etching induced grooves depends only on the size of the LISC zones. Laser ablation is an isotropic process that will sculpt silicon

surface irrespective of the crystallographic orientation [33]. Since the single crystal silicon is isotropic, the refractive index was the same for laser beams propagating in any direction, regardless of the crystallographic orientation. Therefore there is no influence from the light propagation direction with respect to the crystallographic orientation of the wafers on the formation of the LISC zones. Thus the method could be applied to fabricate high-aspect-ratio grooves in silicon wafers with any crystal orientations. Meanwhile, the chemical component of the grooves is only silicon, because the oxygen element was eliminated by the HF acid solution etching. This is of great importance for the silicon-based groove structures' application in micro-fluidics networks, super-hydrophobic microstructures and semiconductor devices.

4. Conclusions

In this paper, the parallel fabrication of all-silicon groove arrays with aspect ratios up to 39.4 were shown via a combination of 800 nm femtosecond laser irradiation and HF acid selective etching. By using a DOE, the processing efficiency was increased by five times. All-silicon grooves were produced due to the chemical reaction of the HF acid solution and SiO_x in the LISC zones. Furthermore, high-aspect-ratio grooves with similar morphologies were fabricated in (100), (110) and (111) silicon wafers by this method, respectively. The method is universally applicable for fabricating high-aspect-ratio deep grooves in various crystal-oriented silicon wafers. Due to the superiority of the simple technological process, the high processing efficiency, the low manufacturing cost, and the single chemical component of the grooves, this method would have potential application in the fabrication of silicon-based advanced functional structures, such as silicon trench capacitors and microfluidic devices.

Acknowledgments

This work was supported by the Collaborative Innovation Center of Suzhou Nano Science and Technology. The authors gratefully acknowledge the financial support for this work which was provided by the National Basic Research Program of China (973 Program) under Grant No. 2012CB921804, the National Natural Science Foundation of China (NSFC) under the Grant Nos. 11204236 and 61308006, and the China Post-doctoral Science Foundation funded project under Grant No. 2013M542315. The authors also sincerely thank Ms Dai at the International Center for Dielectric Research (ICDR) in Xi'an Jiaotong University for her help in using SEM and EDS.

References

- [1] McAuley S A *et al* 2001 Silicon micromachining using a high-density plasma source *J. Phys. D: Appl. Phys.* **34** 2769–74
- [2] Crawford T H R *et al* 2005 Femtosecond laser micromachining of grooves in silicon with 800 nm pulses *Appl. Phys. A* **80** 1717–24
- [3] Zorba V *et al* 2008 Biomimetic artificial surfaces quantitatively reproduce the water repellency of a lotus leaf *Adv. Mater.* **20** 4049–54
- [4] Wang C *et al* 2010 The thresholds of surface nano-/micro-morphology modifications with femtosecond laser pulse irradiations *Nanotechnology* **21** 075304
- [5] Ong W *et al* 2006 Buried microfluidic channel for integrated patch-clamping assay *Appl. Phys. Lett.* **89** 093902
- [6] Sainiemi L *et al* 2008 Fabrication and fluidic characterization of silicon micropillar array electrospray ionization chip *Sensors Actuators B* **132** 380–7
- [7] Nayak B K *et al* 2011 Efficient light trapping in silicon solar cells by ultrafast laser induced self-assembled micro/nano structures *Prog. Photovolt.* **19** 631–9
- [8] Huang Z *et al* 2006 Microstructured silicon photodetector *Appl. Phys. Lett.* **89** 033506
- [9] Werner T R *et al* 1991 Microlens array for staring infrared imager *Proc. SPIE* **1544** 46–57
- [10] Sarajlic E *et al* 2004 Advanced plasma processing combined with trench isolation technology for fabrication and fast prototyping of high aspect ratio MEMS in standard silicon wafers *J. Micromech. Microeng.* **14** S70–5
- [11] Astrova E V *et al* 2010 Optical properties of 1D photonic crystals fabricated by photo-electrochemical etching of silicon *Appl. Phys. A* **98** 571–81
- [12] Barillaro G *et al* 2009 Optical characterization of high-order 1D silicon photonic crystals *IEEE J. Sel. Top. Quantum Electron.* **15** 1359–67
- [13] Jensen K F *et al* 2006 Silicon-based microchemical systems-characteristics and applications *MRS Bull.* **31** 101–7
- [14] McAuley S A *et al* 2001 Silicon micromachining using a high-density plasma source *J. Phys. D: Appl. Phys.* **34** 2769–74
- [15] Fu Y *et al* 2004 Fabrication of 3D microstructures by 2D slice by slice approaching via focused ion beam milling *J. Vac. Sci. Technol. B* **22** 1672–8
- [16] Tolmachev V A *et al* 2005 1D photonic crystal fabricated by wet etching of silicon *Opt. Mater.* **27** 831–5
- [17] Bengtsson M *et al* 2002 Improved performance in silicon enzyme microreactors obtained by homogeneous porous silicon carrier matrix *Talanta* **56** 341–53
- [18] Dwivedi V K *et al* 2000 Fabrication of very smooth walls and bottoms of silicon microchannels for heat dissipation of semiconductor devices *Microelectron. J.* **31** 405–10
- [19] Liu H *et al* 2008 Acquisition of gated spectra from a supercontinuum using ultrafast optical Kerr gate of lead phthalocyanine-doped hybrid glasses *Opt. Express* **16** 13486–91
- [20] Yan L *et al* 2008 Influence of self-diffraction effect on femtosecond pump-probe optical Kerr measurements *Opt. Express* **16** 12069–74
- [21] Döring S *et al* 2012 Evolution of hole shape and size during short and ultrashort pulse laser deep drilling *Opt. Express* **20** 27147–54
- [22] Wang Z *et al* 2009 Polymer hydrophilicity and hydrophobicity induced by femtosecond laser direct irradiation *Appl. Phys. Lett.* **101** 111110
- [23] Zhang Q *et al* 2010 Nanogratings and nanoholes fabricated by direct femtosecond laser writing in chalcogenide glasses *Opt. Express* **18** 6885–90
- [24] Torchia G A *et al* 2007 Femtosecond laser written surface waveguides fabricated in Nd:YAG ceramics *Opt. Express* **15** 13266–71
- [25] Crawford T H R *et al* 2005 Femtosecond laser micromachining of grooves in silicon with 800 nm pulses *Appl. Phys. A* **80** 1717–24

- [26] Aglyamov S R *et al* 2008 Ultrasound measurements of cavitation bubble radius for femtosecond laser-induced breakdown in water *Opt. Lett.* **33** 1357–9
- [27] Vogel A *et al* 2008 Femtosecond-laser-induced nanocavitation in water: implications for optical breakdown threshold and cell surgery *Phys. Rev. Lett.* **100** 038102
- [28] Ma Y *et al* 2012 Photoinduced microchannels and element change inside silicon by femtosecond laser pulses *Opt. Commun.* **285** 140–2
- [29] Pan A *et al* 2013 Fabrication of high-aspect-ratio grooves in silicon using femtosecond laser irradiation and oxygen-dependent acid etching *Opt. Express* **21** 16657–62
- [30] Bekesi J *et al* 2010 Fast fabrication of super-hydrophobic polypropylene by replication of short-pulse laser structured molds *Appl. Phys. A* **99** 691–5
- [31] Kaakkunen J J J *et al* 2011 Water-assisted femtosecond laser pulse ablation of high aspect ratio holes *Phys. Proc.* **12** 89–93
- [32] Ubara H *et al* 1984 Formation of Si–H bonds on the surface of microcrystalline silicon covered with SiO_x by HF treatment *Solid State Commun.* **50** 673–5
- [33] Abbott M *et al* 2006 Optical and electrical properties of laser texturing for high-efficiency solar cells *Prog. Photovolt., Res. Appl.* **14** 225–35